Extreme wave groups in a wave flume: Controlled generation and breaking onset

CrossMark

Eugeny Buldakov [*], Dimitris Stagonas, Richard Simons

UCL, Department of Civil, Environmental & Geomatic Engineering, Gower Street, London, UK

A R T I C L E   I N F O

Keywords:
Extreme waves
Breaking waves
Wave groups
Wave-flume experiment
Harmonics decomposition

A B S T R A C T

Extreme waves in random seas are usually breaking or close to breaking. Understanding the kinematics and evolution of such waves is important for determining loads on offshore structures. Controlled repeatable generation of realistic breaking waves in wave flume experiments is a difficult but important task. It is rather easy to generate an arbitrary breaking wave, but to the authors' knowledge there is no methodology for accurate generation of a wave group with a pre-defined spectrum related to a modelled sea state with spilling breaking at a prescribed position. Such waves can be used to model extreme breaking waves in a random sea and their interaction with structures. This paper offers such a methodology. The key feature of the method is the application of an iterative focussing procedure to a linearised amplitude spectrum rather than to a full nonlinear spectrum. The linearised spectrum is obtained using a harmonics separation technique and the general derivation of the method is given for an arbitrary number of components. The procedure is applied to generate focussed wave groups with amplitudes increased in small steps until local crest breaking occurs. As a result, the highest non-breaking waves and weakly breaking waves are generated for otherwise identical conditions. The methodology is applied for four different wave spectra of the same peak frequency: JONSWAP, Pierson-Moskowitz, wide and narrow band Gaussian. It is found that steepness of the limiting breaking wave depends strongly on the choice of wave group spectrum. The results demonstrate that neglecting spectral properties of design waves may lead to misrepresentation of their breaking behaviour.

1. Introduction

It was always known to seamen that large waves travel in groups (e.g. Buckley, 2005). Later, analysis of records of sea surface evolution demonstrated that it is usual for several high waves to form a continuous sequence usually called a "wave group". Lindgren (1970) gave a theoretical explanation for this empirical fact. According to his results, an average profile of extreme waves in a random Gaussian sea can be represented by a suitably scaled focussed wave group with a shape proportional to the autocorrelation function of the underlying random process. Boccotti (1982) reproduced this result considering wave crests with elevation asymptotically large compared to the significant wave height of the surrounding random Gaussian sea. Continuation of this work led to development of the quasi-determinism theory (Boccotti, 2000). Tromans et al. (1991) suggested a practical application of focussed wave groups as design waves. This approach is now known as the NewWave model. The theory is confirmed by the extensive analysis of field measurement data (e.g. Phillips et al., 1993a,b; Taylor and Williams, 2002; Christou and Ewans, 2014).

Theoretical analysis and observational evidence show that waves with the highest crests belong to wave groups, which are on average symmetric and crest focussed. It should be noted that even for weakly nonlinear sea states, the extreme wave groups could be strongly nonlinear and they are the first waves to experience breaking. In many cases, this will be a single event of spilling breaking localised to the central peak of the wave group. Peak-focussed steep wave groups without breaking or with breaking are therefore good candidates for design waves representing individual extreme events in random seas and their generation in a wave flume is important for experimental investigation of wave-structure interaction, which forms an essential part of the design process of marine structures. To the best of authors' knowledge, using wave groups as design waves is not a commonly agreed industrial practice. However, usefulness of wave groups has started being recognised by practising engineers (e.g. Sutherland and Evers, 2013) and recommendations for their application are finding their way into codes for practice (DNV, 2010).

Wave groups have become a frequent object of study in wave-flume experiments (Baldock et al., 1996; Baldock and Swan, 1996). They are often used as input waves in experimental studies of wave-structure interaction (Swan et al., 1997). To achieve wave focussing at a particular location of a wave flume, various iterative techniques are often used in wave-flume experiments. First application of such a technique is due to Baldock and Swan (1996) and Baldock et al. (1996) who used linear wave theory to calculate phases of different components in a wave group. It was found that the non-linear wave-wave interactions produce a downstream shifting of the focused wave group. This shifting was removed by an iterative procedure in which the nominal value of the focal position in a linear wave group was adjusted until the focus position occurred at the required position. This simple and effective approach relies on using a linear dispersion relation and therefore can not provide perfect focussing for strongly nonlinear wave groups, especially those with long-tailed spectra, when non-linear dispersion plays an important role. The method also can not be easily applied when the dispersion relation is not known *a priory*, e.g. for waves on currents with complex profiles or waves over complex bathymetry. In a more flexible iterative approach phases of the wave generator input are corrected individually to achieve the desired phases of surface elevation time history at a given flume location (e.g. Chaplin, 1996). To generate more complex irregular wave sequences the iteration scheme was extended to include amplitude corrections (Schmittner et al., 2009). This type of iterative technique was successfully applied to generate a wide variety of waves both over complex bathymetry (Fernandez et al., 2014) and over sheared currents (Stagonas et al., 2014).

The accuracy, convergence and overall reliability of iterative focussing techniques reduces considerably with increasing nonlinearity of the wave, which is normally represented by its steepness. The main reason is that the procedure uses a simple iterative technique, which fails when the mapping between the input signal to a wavemaker and the output wave spectrum becomes essentially nonlinear. Phases and amplitudes of input and output are defined for a set of frequency components and it is assumed that an output component depends on an input component of the same frequency. This is generally not true. For example, for a narrow band Gaussian spectrum, higher-order superharmonics of the nonlinear output spectrum are out of the range of the input frequencies. According to this assumption there is no interaction between different frequency components. This assumption neglects nonlinear interaction between spectral components of a wave group. This interaction becomes more important for nonlinear waves and leads to poor convergence of simple iterative techniques for strongly nonlinear steep waves. Another reason for failure of iterative focussing techniques is nonlinear spurious free wave components generated by the wavemaker (e.g. Orszaghova et al., 2014). Such spurious waves are facility dependent and create unpredictable perturbations to the output spectrum.

Difficulties with generation of nonlinear wave groups affect our ability to achieve controlled generation of breaking waves since such waves by their nature are strongly nonlinear. It is relatively easy to generate *a breaking wave* simply by increasing the input amplitude of a previously generated non-breaking wave group. However, there is a serious lack of control over a wave group spectrum, breaker position, its type and intensity. Studies of breaking wave groups often adopt a wave spectrum chosen for the convenience of wave generation. This spectrum may differ from that of a real sea (e.g. Rapp and Melville, 1990; Tian et al., 2012). In engineering experimental studies of breaking wave impact on structures, it is usual to use a strongly breaking wave with a breaker size comparable with the height of the wave (e.g. Chella et al., 2012). High-crested waves with localised spilling breakers, which are more usual in real storms, are very rarely, if ever, used in such experiments.

In this paper we develop an improved iterative focussing methodology. This allows better control over the generated wave group for steep waves. We then use the new methodology to generate a range of steep non-breaking and breaking wave groups of different realistic spectra. The principal feature of the proposed method is the application of an iterative focussing technique not to a fully nonlinear wave record but to a linearised signal obtained by applying spectral decomposition to a nonlinear signal. The spectral decomposition– also called harmonics separation– is a powerful method of analysis of nonlinear wave records and allows separation of harmonics corresponding to different orders of Stokes expansion. The method uses a suitable linear combination of several wave records with appropriate constant phase shifts $\Delta\phi$. For example, half-sums and half-differences of peak ($\Delta\phi = 0$) and trough ($\Delta\phi = \pi$) focussed waves give even and odd harmonics of the signal (Borthwick et al., 2006; Orszaghova et al., 2014). Even terms include second-order super- and sub-harmonics while odd terms include the first-order (or linear) harmonics perturbed by the presence of third- and higher-order odd superharmonics. Including slope focussed waves with $\Delta\phi = \pi/2$ and $\Delta\phi = 3\pi/2$ (Fitzgerald et al., 2014) allows more efficient separation of harmonics. The linearised signal in this method is perturbed by fifth-order terms, which are usually very small.

The structure of the paper is as follows. First, in Section 2 we discuss the method of spectral decomposition, which plays an important role in our wave focussing procedure. We present the general derivation of the method for an arbitrary number of separated harmonics and without assuming small amplitude. Next, Section 3 presents details of the improved wave focussing methodology. Then, Section 4 describes the experimental setup and experimental cases. In Section 5 we present experimental results for steep non-breaking and breaking wave groups. Finally, in Section 6 we discuss results and give concluding remarks.

2. Spectral decomposition

A wave record obtained by a wave probe at a certain location in a wave flume can be considered as the result of a nonlinear transform between an input signal driving a wave maker and an output signal represented by this record. Both input and output can be expressed as complex-valued functions in the form of a complex spectrum obtained by applying a complex Fourier transform to the corresponding time series. We introduce a model representation of such a transform, which represents its principal properties: nonlinearity and dependence of each output spectral component from the entire set of input components. Let an output spectral component $s(\omega)$ at a frequency ω be

$$s(\omega) = \mathcal{F}(\mathcal{L}(S(\Omega;\, \omega));\, \omega),$$

where $\mathcal{L}$ is a linear operator transforming the input spectrum $S(\Omega)$ to a single complex value $z = \mathcal{L}(S)$ and $\mathcal{F}(z)$ is a complex-valued nonlinear function applied to the output of $\mathcal{L}$. Both $\mathcal{L}$ and $\mathcal{F}$ depend on the output frequency ω as a parameter. If a function $\mathcal{F}(z)$ is analytic at $z = 0$ it can be expanded to a converging series

$$s = a_0 + a_1\, z + a_2\, z^2 + a_3\, z^3 + \cdots \tag{1}$$

for values of z inside the convergence circle of $\mathcal{F}$. Let us multiply the input spectrum by a series of complex coefficients $e^{n(2\pi i/N)}, n = 0, 1, ..., N-1$ corresponding to N constant phase shifts $\Delta\phi = 0,\, 2\pi/N,\, 4\pi/n, ...,\, (N-1)\, 2\pi/N$. The same multipliers can be applied to z because the operator $\mathcal{L}$ is linear. Then outputs for phase-shifted inputs can be calculated using expansion (1)

$$
\begin{aligned}
s_0 &= a_0 + a_1\, z + a_2\, z^2 + \cdots + a_{N-1}\, z^{N-1} + \cdots;\\
s_1 &= a_0 + e^{\frac{2\pi i}{N}} a_1\, z + e^{2\frac{2\pi i}{N}} a_2\, z^2 + \cdots + e^{(N-1)\frac{2\pi i}{N}} a_{N-1}\, z^{N-1} + \cdots;\\
&\cdots\\
s_{N-1} &= a_0 + e^{(N-1)\frac{2\pi i}{N}} a_1\, z + e^{2(N-1)\frac{2\pi i}{N}} a_2\, z^2 + \cdots +\\
&\quad + a_{N-1}\, e^{(N-1)^2\frac{2\pi i}{N}} z^{N-1} + \cdots;\\
&\cdots .
\end{aligned}
\tag{2}
$$

Expansions (2) are N-periodic in both vertical and horizontal directions, that is, the expansion s_N is the same as s_0 and coefficients in front of $a_n z^n$ start repeating from the N-th term. Truncating (2) at s_{N-1} and z^{N-1} one can recognise (2) as a set of linear equations with unknowns $a_n z^n$. Solving them makes it possible to calculate individual nonlinear components of the output. Due to a truncation error, solution for a component n will also include components $n + N$, $n + 2N$, etc. However, for a converging series, the contribution of higher-order components rapidly decreases with increasing N. For $N = 2$ (2-waves decomposition) we have

$$a_0 + a_2 z^2 + \cdots = (s_0 + s_1)/2 \, ;$$
$$a_1 z + a_3 z^3 + \cdots = (s_0 - s_1)/2 \, ,$$

which corresponds to the classical half-difference and half-sum of peak- and trough-focussed waves used for separating odd and even components (Borthwick et al., 2006; Orszaghova et al., 2014). For $N = 4$ (4-waves decomposition) we have

$$a_0 + a_4 z^4 + \cdots = (s_0 + s_1 + s_2 + s_3)/4 \, ;$$
$$a_1 z + a_5 z^5 + \cdots = (s_0 - i\,s_1 - s_2 + i\,s_3)/4 \, ;$$
$$a_2 z^2 + a_6 z^6 + \cdots = (s_0 - s_1 + s_2 - s_3)/4 \, ;$$
$$a_3 z^3 + a_7 z^7 + \cdots = (s_0 + i\,s_1 - s_2 - i\,s_3)/4 \, .$$

This type of decomposition allows efficient separation of components (e.g. Fitzgerald et al., 2014) and we use it in this paper. Fig. 1 shows an example of application of the 4-waves decomposition to our experimental results and demonstrates clear separation of spectral components of the decomposed signal. Higher-order decompositions are possible, but they significantly increase the amount of required experimental work. Applicability of the method is restricted by convergence of (1) and requires further study. However, results of this paper demonstrate practical applicability of the method for non-breaking waves and for waves with weak localised breaking.

A considerable advantage of using spectral decomposition for analysis of experimental wave group records is convenience of separation of wave components of physical interest from components caused by imperfections of wave generation. The former include the first order free component and bound higher order components and the latter include higher-order spurious free waves. We should note that spurious free waves depend on the particular type of wavemaker and complicate direct comparison of results from different facilities. Fig. 2 shows an example of decomposition of a wave record at the focus position $x = 0$ in the middle of the tank for one of the wave groups considered in the paper. Vertical lines indicate theoretical times when the corresponding wave group component arrives at the focus location. It is assumed that each wave component travels through a flume of half-length $L = 6.5$ m with an appropriate linear group velocity U. Velocity $U_1 = 0.894$ m/s corresponding to a peak frequency $f_p = 1$ Hz is used for first-order free components and for all bound components. Second-order high frequency

spurious free waves travel with the velocity $U_2 = 0.390$ m/s corresponding to the double peak frequency. Second-order low frequency spurious components travel with the long wave velocity $U_0 = 1.981$ m/s. Arrows show directions of time shifts of the corresponding wave groups when the wave probe moves in the main direction of wave propagation.

The top plot of Fig. 2 shows first-order incoming and reflected waves. The latter arrive at the centre of the flume with the time delay $2\,L/U_1$. As can be seen from the middle plot, the bound high-frequency second-order component travels together with the first-order wave. The corresponding spurious free component travels with the lower velocity U_2 and arrives at the centre of the flume with the delay $L/U_2 - L/U_1$. It is difficult to separate bound and free components for second-order sub-harmonics. Therefore, on the lower plot we subtract the minus term of an analytical second-order wavegroup solution from the full signal. The remaining part of the signal shows a low-frequency spurious free wave in the form of a small solitary wave. This wave travels faster than the main first-order wave group and arrives at the centre of the flume before the main group at a time $L/U_0 - L/U_1$. The reflected low-frequency component arrives after the main group at a time $L/U_0 - L/U_1 + 2\,L/U_0$. It can be seen that separation of low-frequency components from the full signal is difficult and requires either a second-order wave generation system or a very long flume.

3. Wave generation methodology

We use the following iterative procedure to generate waves of a pre-selected target spectrum

$$a_{\text{in}}^n(f_i) = a_{\text{in}}^{n-1}(f_i)\, a_{\text{tgt}}(f_i)\big/a_{\text{out}}^{n-1}(f_i);$$
$$\phi_{\text{in}}^n(f_i) = \phi_{\text{in}}^{n-1}(f_i) + \big(\,\phi_{\text{tgt}}(f_i) - \phi_{\text{out}}^{n-1}(f_i)\,\big)\, , \tag{3}$$

where $a_{\text{in}}^n(f_i)$ and $\phi_{\text{in}}^n(f_i)$ are the amplitude and phase of an input spectral component at frequency f_i for n-th iteration; $a_{\text{out}}^n(f_i)$, $\phi_{\text{out}}^n(f_i)$ are amplitudes and phases of the corresponding spectral components of the recorded output spectrum and $a_{\text{tgt}}(f_i)$, $\phi_{\text{tgt}}(f_i)$ are target spectral components. Equation (3) can be considered as an iterative solution of a complex-valued optimisation problem calculating a complex input spectrum $s_{\text{in}} = a_{\text{in}}\exp(\phi_{\text{in}})$ of a nonlinear transfer function, which generates a prescribed output spectrum. Equation (3) are general and can be applied to various physical input and output spectra connected by various physical processes defining a transfer function between input and output. We use a linearised surface elevation spectrum obtained by the 4-wave decomposition described in the previous section as an output of the iterative process (3).

Using a linearised signal instead of a fully nonlinear signal as an output of an iterative focussing process considerably reduces nonlinearity of the transfer function between the wavemaker input and the recorded output. Bound higher-order components are removed from the consideration. This has a clear positive effect on convergence of the
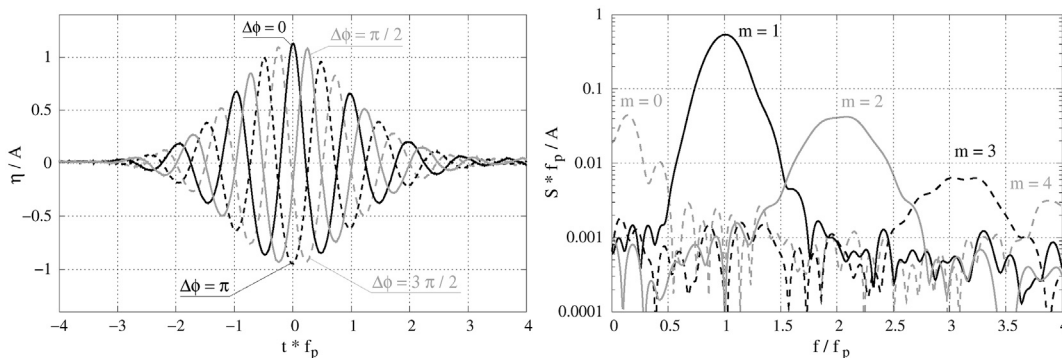

Fig. 1. Spectral decomposition of surface elevation signal at $x = 0$ for case GN1. Left: synchronised signals with different phase shifts $\Delta\phi$. Right: The decomposed spectra for components corresponding to different terms m of the expansion (1).
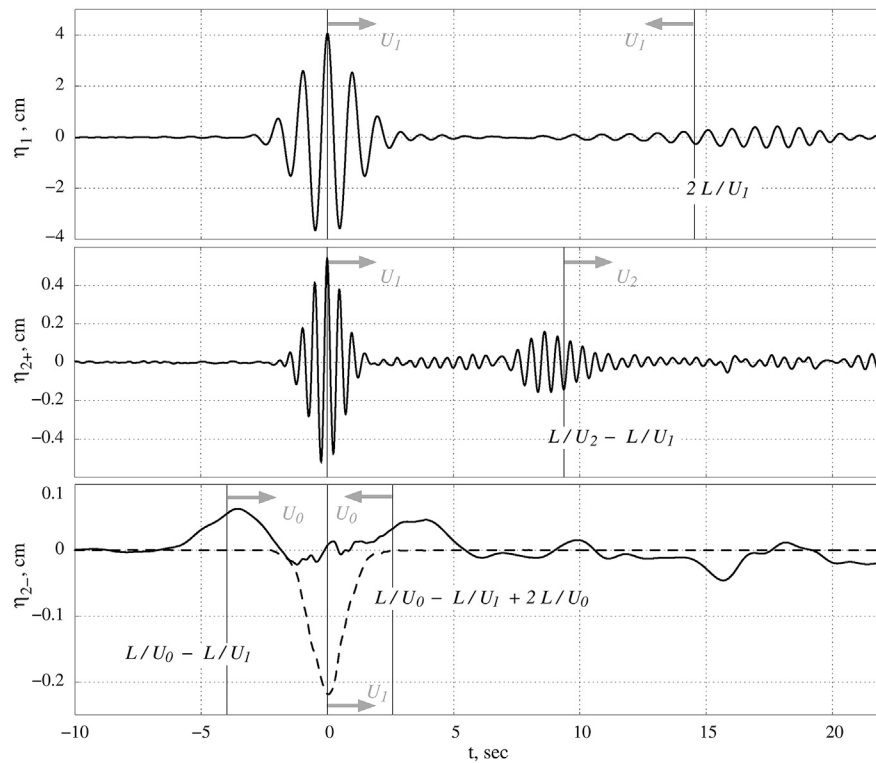
Fig. 2. Decomposed time histories of surface elevation at focus ($x = 0$). Case GN1. Top: first-order component. Middle: high-frequency second-order component. Bottom: low-frequency second-order component showing an analytical solution for a bound wave (dashed) and the rest of the signal (solid).

iterative procedure. Nonlinear spurious free harmonics including second-order sub-harmonics can also be filtered from the output. As can be seen from Fig. 2, high-frequency free components can be removed from the output signal by selecting a suitable time window without applying the spectral decomposition This approach is inefficient for low-frequency free components. However, if a linearised signal is used for iterations, the time window can be selected to include a wave group without reflections and spurious components. This contributes to better control over wave group generation and improves convergence of the iterative focussing.

The second key feature of the suggested methodology is using wave records at different positions for phase and amplitude iterations. When a steep wave group travels along a flume, its linearised amplitude spectrum changes due to nonlinear interaction between individual modes. Matching an amplitude spectrum with a target far away from the wavemaker requires generation of a wave with a non-physical initial spectrum, which approaches a meaningful target as the wave travels to the focussing position. For example, for a spectrum without a high frequency tail, e.g. Gaussian, nonlinear modal interactions lead to energy transfer from lower to higher frequencies of the spectrum. Generating such a spectrum far from the wavemaker requires a reduction in the amplitudes of higher frequency components. This leads to insufficient control over both amplitudes and phases of these components when the corresponding amplitudes becomes too small. In addition, there is considerable viscous dissipation of high frequency components. This leads to generation of a non-physical wave spectrum near the wavemaker with energy excess at high frequencies. We found it useful to match the amplitude spectrum of the generated wave with the target well before the focussing position, relatively close to the wavemaker. The amplitude spectrum of the wave group develops naturally, as it travels towards the phase focus location. This improves stability and convergence of iterations. There is also a deep physical reason for selection of an amplitude matching point in front of the phase focus position. Waves generated in such a manner reproduce natural features developed by real extreme waves after their emergence from the surrounding random sea. The

NewWave theory is valid for linear waves. Therefore, when one selects a sea state spectrum as a wave group amplitude spectrum, the spectrum applies to a wave group before its linearised spectrum has been changed by nonlinear interaction of spectral components. This is the case for an unfocussed wave group far in front of the focus location, where its surface elevation is small and it can be considered linear. Therefore, when one generates a wave group in a wave-flume experiment, it would be appropriate to select the amplitude matching position as far away from the phase focus position as possible. On the other hand, the distance between the amplitude matching position and the wavemaker should be large enough to exclude influence of exponential evanescent modes. It should also be noted, that the presented approach does not rely on a wavemaker control system to generate a wave with a specified spectrum at the paddle position, like some early methods. The amplitude matching position is selected by an experimentalist from required test conditions. For example, the amplitude matching position can coincide with the focussing position, if the direct control of a generated amplitude spectrum is required. This could be appropriate if the actual shape of the linearised amplitude spectrum at the focal position after its nonlinear evolution is known *a priori*.

The focussing methodology consists of the following steps. First, we select an initial approximation to the input spectrum and generate waves using this input with four phase shifts $\Delta\phi = 0$, $\pi/2$, π, $3\pi/2$. Surface elevation of the resulting waves is recorded at a target location (phase focussing position) and at a position far in front of it (amplitude matching position). As discussed above, the latter should be as far from the former as possible, and far enough from the wavemaker to exclude the influence of non-oscillating exponential evanescent modes. Then, 4-waves spectral decomposition is applied to the recorded spectra. The first-order decomposed amplitude spectrum at the amplitude matching position is used as a_{out}^0 and first-order phases of the decomposed spectrum at the phase focussing position are used as ϕ_{out}^0. Substitution into (3) produces a corrected input spectrum (a_{in}^1, ϕ_{in}^1), which is used as wavemaker input in the next iteration. The procedure is repeated either until the desired

accuracy of the output is achieved or until iterations stop converging.

It should be noted that the methodology (as with any empirical iterative focussing methodology) does not depend on any particular transfer function of the wavemaker control system used to generate paddle motion from an input spectrum. This ensures flexibility of the methodology. For example, if a wavemaker control system uses the time history of the paddle displacement as an input, one can calculate a spectrum of displacement and use it as an input in the iterative procedure. If the iterations converge, the procedure will produce the same resulting wave as for a control system using input spectrum directly.

4. Experimental setup, procedures and cases

Experiments on generation of focussed nonlinear wave groups were performed in the coastal wave flume in the Civil Engineering Department at UCL. The flume has the width of 45 cm and the length of the working section between 2 piston wavemakers is 13 m. The wavemaker at one end of the flume is used for wave generation and the opposite one for active reflection absorption. Wave groups were focussed at the midpoint along the flume. The focus location is used as the origin of the coordinate system with the x-axis directed towards the generating paddle. The x-coordinate of the wave generator is therefore $x_{wm} = 6.5$ m and a generated wave propagates in the negative direction towards the focus location $x = 0$. Water depth over the horizontal bed was set to $h = 0.4$ m. Wave propagation was monitored by a series of resistance wave probes measuring time history of surface elevation at several positions along the flume. Records of surface elevation at $x = 0$ were used for phase focussing and records at the position $x = 5$ m for amplitude spectrum matching.

The control system of the paddles operates in the frequency domain. It uses discrete spectra to generate periodic paddle motions. For our experiments, we use an overall return period of 128 s. This is the time between repeating events generated by the paddle. The range of frequencies used in the experiments was from $1/128$ Hz to 4 Hz with 512 equally spaced discrete frequency components with a step of $1/128$ Hz. Each wave spectrum was generated 4 times with constant phase shifts $\Delta\phi = \pi n/2$, $n = 0, 1, 2, 3$ added to all frequency components of an input spectrum. Then, a complex Fourier transform was used to calculate values of phases and amplitudes for the same discrete set of frequencies that is used for wave generation. The decomposition procedure was then applied to separate 4 sets of harmonics. The first-order amplitude spectrum at $x = 5$ m was used as an amplitude output and the first-order phase spectrum at $x = 0$ as a phase output to organise focussing iterations.

We must emphasise the importance of synchronisation between the 4 phase-shifted wave records. Even small de-synchronisation may lead to considerable decomposition errors. We found that the required synchronisation level is within $1/100$ of a typical wave period. In this study, we tested 2 synchronisation methods: hardware and post-processing synchronisation. The post-processing synchronisation is achieved in the following way. First, we calculate phase spectra of four phase-shifted signals $\Delta\phi_n = \pi n/2$, $n = 0, 1, 2, 3$. Then, values of phases for each spectrum are changed by $2\pi M$, where a whole M is selected to minimise the absolute value of the phase for the spectral peak frequency $\phi_n(\omega_p)$. This gives the actual value of the phase shift at the peak frequency for each of the four waves. We denote this value $\tilde{\Delta}\phi_n$. The synchronising time shift for each wave is then calculated as $\Delta t = (\Delta\phi_n - \tilde{\Delta}\phi_n)/\omega_p$. The procedure ensures that the values of phases at peak frequency have accurate values of phase shifts and the resulting four signals are well synchronised. The post-processing synchronisation demonstrated good results and can be recommended when hardware synchronisation of sufficient precision is not available. However, hardware synchronisation used in our experiments had acceptable accuracy and results presented in this paper are obtained using this synchronisation method. It is also important to select an appropriate initial guess of the input spectrum to

ensure faster convergence of iterations (3). This becomes crucial for steep waves when certain inputs can cause serious convergence problems, for example, due to premature breaking of a wave group before it reaches the focus location. On the other hand, for small and moderate waves, convergence is usually very good. We therefore use an iterative procedure with gradually increasing target amplitude. An upscaled input obtained for a smaller amplitude was used to start iterations for a larger one. For sufficiently small amplitude steps, this provides good initial inputs even for very steep waves.

For test cases, we use 4 types of target spectrum with the same peak frequency $f_p = 1$ Hz: narrow band Gaussian, wide band Gaussian, JONSWAP and Pierson-Moskowitz. Shapes of target spectra can be seen in Fig. 3. The linear phase velocity for waves at this frequency for our depth is $C_1 = 1.46$ m/s, the group velocity is $U_1 = 0.89$ m/s and the wavelength is $\lambda_1 = 1.46$ m $= 3.65h$. We therefore have intermediate depth conditions. After rescaling to water depth of 60 m these conditions correspond to waves with peak period of 12 s, which represents conditions of a typical North-Sea storm. For each spectrum type we start by generating small waves of peak amplitude $A = 2$ cm. The resulting input signals were doubled and further iterations were used to generate moderately nonlinear waves with amplitude $A = 4$ cm. Only 1–2 iterations are required to achieve good focussing of small waves and a further 2–3 iterations were required to focus larger waves. Further increase of wave amplitude was made in small steps individually for each spectral case. For large waves, the number of iterations depends on the particular case and the desired focussing accuracy. For most of the cases, it was possible to achieve acceptable wave quality after 3 iterations. When waves were close to breaking, the amplitude steps were reduced to 10%. The process continued until the first fully focussed wave group with a breaking crest was generated. Breaking was identified visually. This defines breaking limits within 10% of wave amplitude.

Cases selected for demonstration of results and further analysis are presented in Table 1. The first case for each spectrum represents a basic moderately steep wave with a linear focus amplitude 4 cm. Cases 2 and 3 correspond to the largest non-breaking and first breaking waves obtained for each spectrum type. The corresponding values of amplitudes are specific to each spectrum. Column 3 of the table gives values of linear focus amplitudes, which are target amplitudes for the iterative process and are therefore input parameters of wave generation. These amplitudes were achieved by the iterative process with a good accuracy and can be considered as actual linear amplitudes of generated waves. Column 4 of the table gives measured values of maximum surface elevation of peak-focussed waves at the focus position. We should note the special behaviour of the breaking narrow band Gaussian case (Case GN3). Unlike other breaking cases, for this case we did not manage to generate a focussed wave with the crest breaking at the focus location. As will be discussed later, for the case GN3 the wave is not well focussed and breaks downwave of the focus position.

5. Results

Results for the application of the iterative focussing technique are presented in Figs. 3–5. They show spectra, time histories and snapshots of wave profiles for the highest non-breaking and weakly breaking wave groups. For all cases except the narrow band Gaussian, well-focussed steep non-breaking and breaking waves are generated. The breaking crests of peak-focussed waves occur exactly at the focus position (Figs. 4 and 5). A perfect match of the linearised amplitude spectrum at the front wave probe is achieved (Fig. 3). Phase focussing at the focus position is very good for spectral components with sufficiently large amplitudes. For frequencies with small amplitudes, the phases are out of focus. This does not affect wave behaviour because of the smallness of amplitudes of the corresponding spectral components.

For the narrow band Gaussian spectrum, good focussing results are achieved for moderately steep waves (case GN1). For steeper waves, amplitude iterations fail to converge and finally start diverging. The
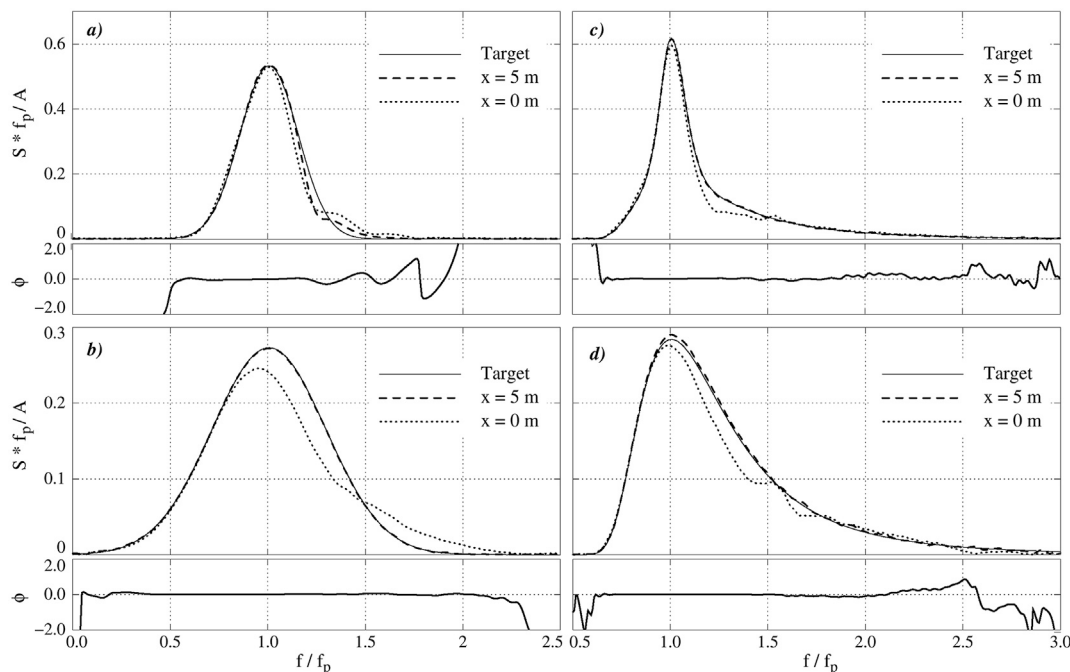
Fig. 3. Linearised spectra for focussed strongly nonlinear wave groups for cases a) GN2, b) GW3, c) JS3 and d) PM3.

Table 1
Experimental cases. For all cases water depth $h = 40$ cm and peak frequency $f_p = 1$ Hz.

Case	Spectrum	Linear focus amplitude, A	Crest elevation at focus, η_c
GN1	Narrow band Gaussian	4.0 cm	4.47 cm
GN2	Narrow band Gaussian	7.6 cm	8.61 cm
GN3	Narrow band Gaussian	7.98 cm	9.39 cm
GW1	Wide band Gaussian	4.0 cm	4.54 cm
GW2	Wide band Gaussian	6.4 cm	8.13 cm
GW3	Wide band Gaussian	6.8 cm	8.97 cm
JS1	JONSWAP	4.0 cm	4.43 cm
JS2	JONSWAP	5.6 cm	6.88 cm
JS3	JONSWAP	6.0 cm	7.28 cm
PM1	Pierson-Moskowitz	4.0 cm	4.44 cm
PM2	Pierson-Moskowitz	4.8 cm	5.42 cm
PM3	Pierson-Moskowitz	5.2 cm	5.79 cm

problem was caused by instability of spectral amplitude components with frequencies around 1.4 Hz (Fig. 3a). We continued increasing wave amplitude and attempted focussing using only phase iterations without correcting the amplitude spectrum. This allowed us to generate a very high (linearised amplitude $A = 7.6$ cm, maximum crest elevation $\eta_c = 8.61$ cm) and relatively well focussed non-breaking wave (Figs. 4 and 5, Case GN2). An attempt to increase the amplitude by a further 5% produced a wave group which starts defocussing at $x = 0$ (Figs. 4 and 5, Case GN3). Wave amplitude grows quickly after the focussing position and the wave breaks intensively further down the flume. The highest total crest elevation $\eta_c = 9.97$ cm measured in all our experiments was recorded for the case GN3 with π phase shift at the position $x = -2$ m along the flume. All other waves observed in our experiments were approximately symmetric with respect to the focus position with maximum elevation achieved by the peak-focussed group (phase shift zero) at the focus position.

The behaviour of the steep wave group with a narrow band Gaussian spectrum can be explained by resonant third-order interactions of the spectral components. It is similar to the behaviour of wave groups with a JONSWAP spectrum during long-term evolution in intermediate water presented by Katsardi and Swan (2011). Our results support the

conclusions of Katsardi and Swan (2011) on the existence of two fundamentally different types of extreme wave events: those produced by dispersive focussing such as predicted by the NewWave model (as for most cases presented in this paper), and those dominated by modular instability caused by resonant interactions (like the case GN3). Dominance of either dispersive focussing or modular instability for a particular wave group depends on the relative time scales of both effects. If a typical time of focussing– and therefore of defocussing– of a wave group is much smaller than a characteristic time of modular instability, the latter will not affect wave group behaviour. Modular instability is controlled by the Benjamin-Feir index (BFI) which is proportional to wave steepness and inversely proportional to the bandwidth of a wavenumber spectrum (e.g. Onorato et al., 2006). Steeper waves of smaller bandwidth are more unstable. Therefore, all the wavegroups presented in this paper apart from GN3, are either stable or weakly unstable with a typical time of instability larger than the focussing time for our flume conditions. On the other hand, the steep narrow band wave group for the case GN3 exhibits strong instability leading to its special behaviour compared to all other cases.

Let us now consider the characteristics of wave groups on the onset of breaking. Table 2 shows various measures of wave steepness and nonlinearity for the highest non-breaking waves (Case 2) and weakly breaking waves (Case 3) for wave groups of different spectra. We exclude the special case of the narrow band Gaussian spectrum from this analysis. Parameters corresponding to breaking onset take values intermediate between cases 2 and 3. First, we introduce the global steepness of the wave group as

$$S = \sum_i a_i k_i,$$

where a_i and k_i are amplitudes and wave numbers of spectral components of the wave group. We calculate the global steepness for linear input spectra (S_L) and for fully nonlinear spectra measured at the focus point (S_{NL}). The linear steepness S_L is a predictive parameter and can be calculated from *a priori* knowledge of wave group linear spectrum and amplitude. This parameter can therefore be used for formulating a kinematic criterion of wave breaking. It is suggested that a wave group breaks if its global steepness S_L is larger than a certain critical value
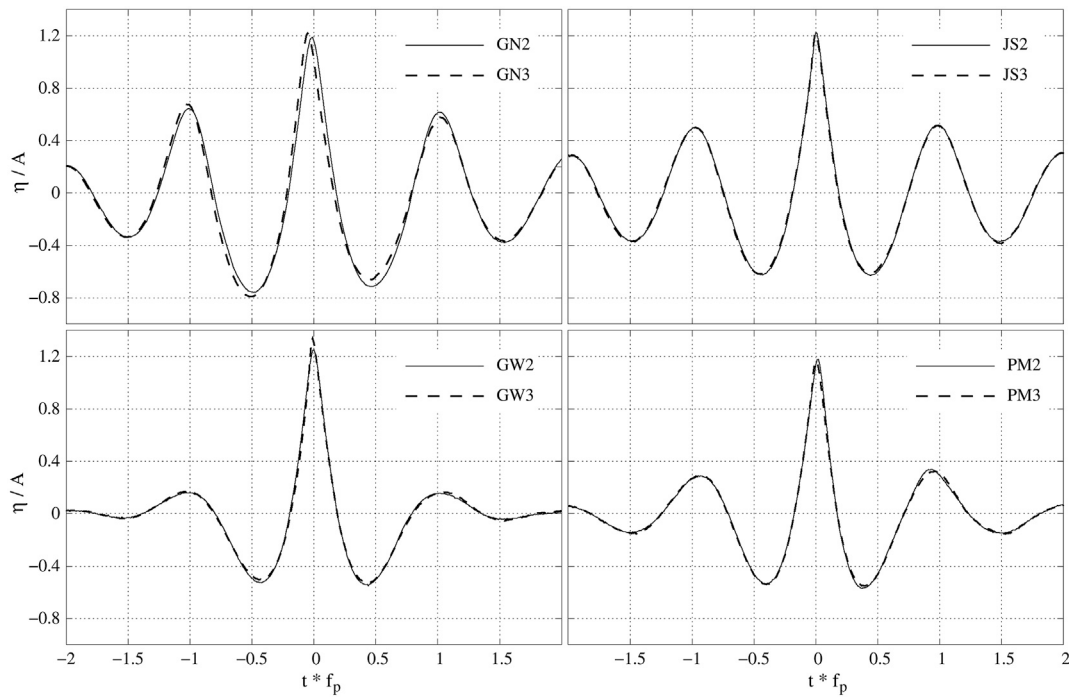
Fig. 4. Fully nonlinear time histories of peak-focussed wave groups of different spectra at $x = 0$ for the highest nonbreaking (solid) and breaking (dashed) cases.
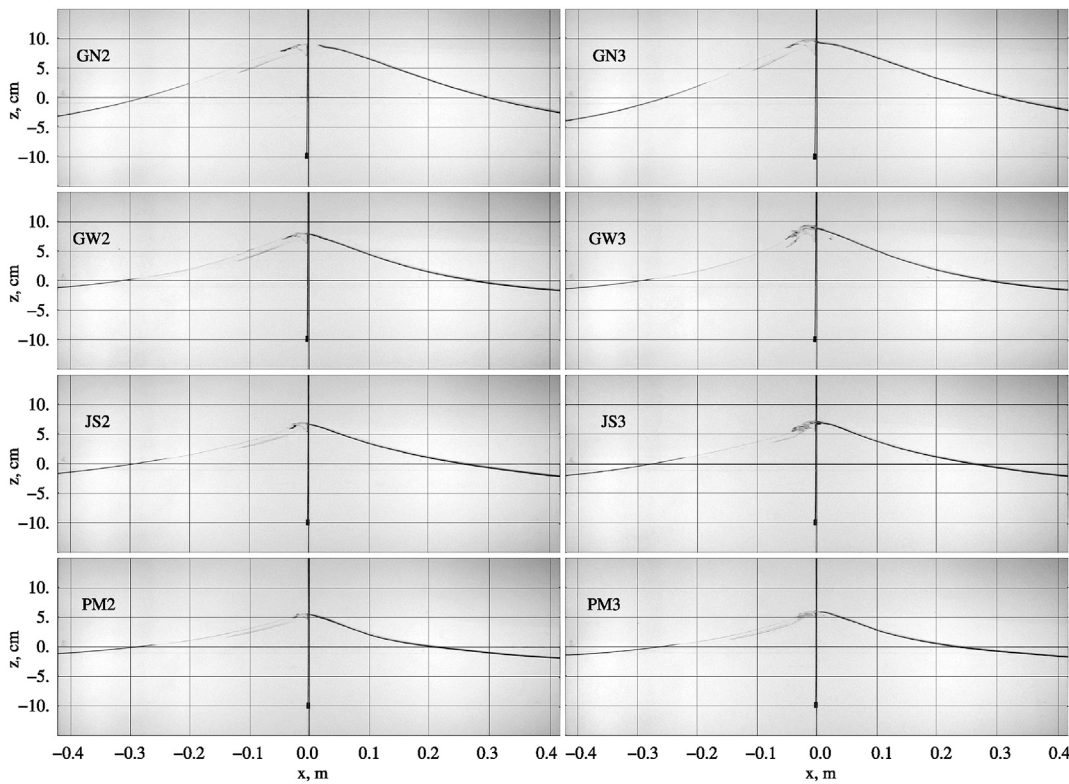

Fig. 5. Snapshots of peak-focussed pre-breaking (left) and breaking (right) wave profiles for wave groups of different spectra. For case GN3 breaking occurs downwave of the focussing position.

(Perlin et al., 2013). For example, Drazen et al. (2008) reported values of S corresponding to spilling breaking onset in the range 0.32–0.36 for a wave group consisting of harmonics of equal steepness with different central frequency and bandwidth. As can be seen from Table 2, values of S_L corresponding to the onset of breaking do not change much for

different spectra and are close to the values reported by Drazen et al. (2008). However, small differences in critical values of S_L for different spectra do not allow to use them as a universal breaking criterion.

A fully nonlinear global steepness S_{NL} results from nonlinear evolution of a wave group. It is calculated from the actual surface elevation at

Table 2
Steepness for the highest non-breaking (Case 2) and weakly breaking (Case 3) peak focussed waves groups of different spectra. S_{NL} – global steepness for full nonlinear spectrum; S_L – global steepness for linear target spectrum; s_c – local crest steepness; ξ – nonlinear growth of crest elevation.

	Case 2				Case 3			
	S_L	S_{NL}	s_c	ξ	S_L	S_{NL}	s_c	ξ
GW	0.32	1.04	0.0142	0.27	0.34	1.21	0.0156	0.32
JS	0.38	0.91	0.0127	0.23	0.40	0.98	0.0136	0.21
PM	0.38	0.77	0.0110	0.13	0.40	0.81	0.0119	0.11

the focus location obtained from experimental or numerical modelling. Therefore, this parameter has limited predictive power, but illustrates actual behaviour of a wave group at focus. As can be seen from Table 2, the value of S_{NL} depends strongly on the wave spectrum. Global steepness of the breaking onset reduces considerably for wave groups with greater relative contribution of spectral components at the high frequency tail of a spectrum. To explain this behaviour let us consider local crest steepness defined as $s_c = \eta_c/b$, where b is the width of the crest at the mean water level, and relative growth of crest elevation due to nonlinearity $\xi = (\eta_c - A)/A$. Both these parameters exhibit similar behaviour to the fully nonlinear global steepness. Their values corresponding to the breaking onset decrease for spectra with greater contribution from high frequency components. Focussing of high frequency components leads to high curvature of the free surface in close vicinity to a wave crest. This creates a localised region of strong nonlinearity resulting in breaking. The larger contribution from high frequencies causes stronger local nonlinearity and leads to breaking at smaller wave steepness and smaller nonlinear growth of crest elevation. These results demonstrate that the practically important parameters of a breaking wave such as crest steepness and maximal crest elevation depend strongly on wave spectrum. Neglecting the spectral properties of the waves groups used as design waves may lead to misrepresentation of their breaking behaviour.

6. Concluding remarks

The central result of the paper is an improved focussing methodology capable of generating very steep focussed wave groups with and without breaking. The method offers an opportunity to study the properties of steep waves and the physics of spilling breaking. Accurate reproduction of a linearised wave amplitude spectrum at a specified flume position for a wide range of amplitudes allows a proper parametric study of steep wave groups since increasing amplitude does not change the shape of the spectrum. For example, Fig. 4 demonstrates identical scaled wave records for breaking and non-breaking waves. Comparison of similar waves with and without breaking gives a useful tool to study the effects of breaking on overall wave evolution. In this paper we study peak-focussed waves as a representation of extreme waves suggested by the NewWave theory and as the highest waves for a given amplitude spectrum. However, the

method is not restricted by peak-focussed waves and can be applied equally to any target phase distribution.

As a step in the methodology development, we revisited the spectral decomposition technique. We presented a new derivation of the method, which does not assume small wave amplitude and does not use Stokes expansion as a particular form of solution. Our derivation is therefore more general. We consider an arbitrary number of separated modes equal to the number of waves used in the decomposition and present the general method for obtaining decomposition equations. Results presented in the paper demonstrate that the decomposition method can be applied successfully for all non-breaking waves and for waves with weak localised breaking.

An essential advantage of the methodology presented in this paper is its independence of a particular form of the transfer function between the wavemaker input and the recorded wave output. An important practical consequence of this property is the ability of the method to reproduce results in different facilities and at different scales. This allows the study of effects not scaled by the Froude law, such as surface tension, aeration and viscous dissipation, which affect the breaking process. To demonstrate the scalability of the methodology and its transferability to different experimental facilities some cases were reproduced in a larger wave flume at HR Wallingford. The flume is 60 m long and is equipped with a flap wavemaker. The depth was set to $h = 1.6$ m and the corresponding Froude-scaled peak frequency was $f_p = 0.5$ Hz. Positions of wave probes were scaled accordingly. The amplitude matching probe was placed at a position 20 m in front of the phase focussing probe. Fig. 6 shows perfect comparison between first-order wave components and a good comparison between second-order super- and sub-harmonics. The method is also independent from a specific form of a dispersion relation. This allows its application over variable bathymetry provided depth variations are moderate and do not lead to strong reflections and breaking before the focussing position.

A disadvantage of the proposed methodology is the necessity to generate multiple waves before applying spectral decomposition technique. To reduce the required number of experimental runs it is possible to use an original iterative procedure without spectral decomposition for small amplitude waves. For moderately high waves, it can be sufficient to use 2-waves decomposition using only peak- and trough-focussed waves. For the highest waves it is however essential to apply the full version of the method with 4-waves decomposition. For larger facilities it is advisable to use a numerical wave tank for iterative focussing as, for example, suggested by Fernandez et al. (2014), and then to apply final iterations in the facility. When an input signal is created, it can be used to reproduce this wave in future experiments, including those with structures.

An important application of the method is generating incoming waves in experimental studies of wave-structure interaction. The method offers a useful opportunity to study breaking effects on wave-structure interaction. Comparison of loads created by identical wave groups with and
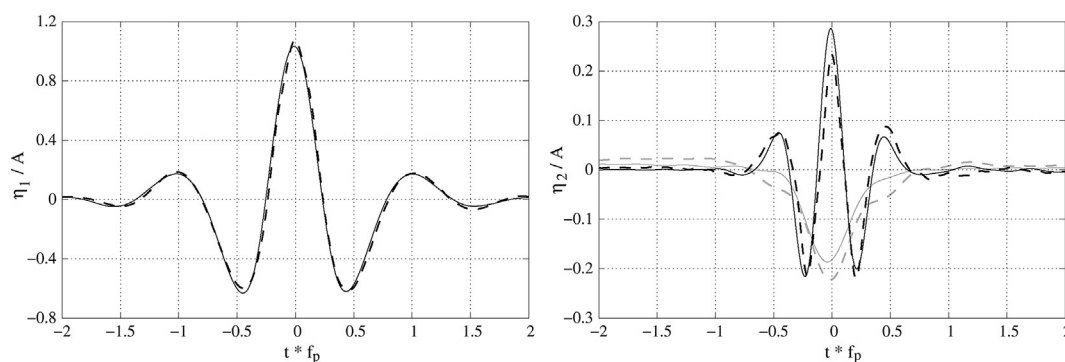
Fig. 6. Comparison of surface elevation at the focus location for waves generated in different facilities. Solid: Original case GW2, piston wavemaker. Dashed: Case GW2 rescaled for depth $h = 1.6$ m, flap wavemaker. Other scaled parameters are $f_p = 0.5$ Hz, $A = 25.6$ cm. Left: first-order component. Right: second-order superharmonics (black) and subharmonics (grey).

without breaking allows identification of loads associated with breaking and their detailed investigation. An important challenge is to find a phase distribution for a wave group with a given amplitude spectrum, which would generate a maximum load on a specific structure. For a given amplitude spectrum, peak-focussed wave groups considered in this paper produce maximum velocities under the high crest. Such waves impose maximum loads on drag-dominated structures. Our method also requires the generation of slope focused waves associated with the highest accelerations and applying maximum loads on inertia-dominated structures. In the general case, a phase distribution associated with maximum load is not known *a priori*. A possible method for producing a wave group with a given amplitude spectrum, which generates a maximum load, is to solve an optimisation problem maximising the load predicted by a simple wave-structure interaction model, for example, by Morison's equation with linear wave model. The predicted spectrum can then be used as a target spectrum for the iterative procedure. The wave group created by this method will generate a load, which will be close to the maximum, with an error caused by imperfection of the predictive model. Another method follows from the invariance of the iterative methodology to the transfer function relating input and output. One can use a load record as instead of a surface elevation record as the output. In linear approximation, the maximum load occurs when the phases of all load spectral components are zero. The iterative procedure can be applied to the linearised load spectrum to produce wave input which generates the linearised load spectrum with zero phase distribution. The resulting wave group will generate the structural load close to maximum with a small error caused by the nonlinearity of the wave-structure interaction process.

Acknowledgments

References

Baldock, T., Swan, C., Taylor, P., 1996. A laboratory study of nonlinear surface waves on water. Philos. Trans. Roy. Soc. A Math. Phys. Eng. Sci. 354 (1707), 649–676.

Baldock, T., Swan, C., 1996. Extreme waves in shallow and intermediate water depths. Coast. Eng. 27, 21–46.

Boccotti, P., 1982. On ocean waves with high crests. Meccanica 17 (1), 16–19.

Boccotti, P., 2000. Chapter 9: the theory of quasi-determinism. In: Boccotti, P. (Ed.), Wave Mechanics for Ocean Engineering, Elsevier Oceanography Series, vol. 64. Elsevier, pp. 281–309.

Borthwick, A., Hunt, A., Feng, T., Taylor, P., Stansby, P., 2006. Flow kinematics of focused wave groups on a plane beach in the U.K. coastal research facility. Coast. Eng. 53 (12), 1033–1044.

Buckley, W.H., 2005. Extreme Waves for Ship and Offshore Platform Design: an Overview. in: Design and Operation for Abnormal Conditions III. The Royal Institution of Naval Architects, London.

Chaplin, J., 1996. On frequency-focusing unidirectional waves. Int. J. Offshore Polar Eng. 6 (2), 131–137.

Chella, M., Tørum, A., Myrhaug, D., 2012. An overview of wave impact forces on offshore wind turbine substructures. Energy Procedia 20, 217–226.

Christou, M., Ewans, K., 2014. Field measurements of rogue water waves. J. Phys. Oceanogr. 44 (9), 2317–2335.

DNV, October 2010. Recommended Practice: Environmental Conditions and Environmental Loads. DNV-RP-C205. Det Norske Veritas, Norway, Ch. 10.7.4 Testing in Single Wave Groups, p. 107.

Drazen, D.A., Melville, W.K., Lenain, L., 2008. Inertial scaling of dissipation in unsteady breaking waves. J. Fluid Mech. 611, 307–332.

Fernandez, H., Sriram, V., Schimmels, S., Oumeraci, H., 2014. Extreme wave generation using self correcting method – revisited. Coast. Eng. 93, 15–31.

Fitzgerald, C., Taylor, P., Eatock Taylor, R., Grice, J., Zang, J., 2014. Phase manipulation and the harmonic components of ringing forces on a surface-piercing column. Proc. Roy. Soc. A Math. Phys. Eng. Sci. 470 (2168).

Katsardi, V., Swan, C., 2011. The evolution of large non-breaking waves in intermediate and shallow water. I. Numerical calculations of uni-directional seas. Proc. Roy. Soc. A Math. Phys. Eng. Sci. 467, 778–805.

Lindgren, G., 1970. Some properties of a normal process near a local maximum. Ann. Math. Stat. 41 (6), 1870–1883.

Onorato, M., Osborne, A., Serio, M., Cavaleri, L., Brandini, C., Stansberg, C., 2006. Extreme waves, modulational instability and second order theory: wave flume experiments on irregular waves. Eur. J. Mech. B/Fluids 25 (5), 586–601.

Orszaghova, J., Taylor, P.H., Borthwick, A.G., Raby, A.C., 2014. Importance of second-order wave generation for focused wave group run-up and overtopping. Coast. Eng. 94, 63–79.

Perlin, M., Choi, W., Tian, Z., 2013. Breaking waves in deep and intermediate waters. Annu. Rev. Fluid Mech. 45, 115–145.

Phillips, O., Gu, D., Donelan, M., 1993a. Expected structure of extreme waves in a Gaussian sea. Part I: theory and SWADE buoy measurements. J. Phys. Oceanogr. 23 (5), 992–1000.

Phillips, O., Gu, D., Walsh, E., 1993b. On the expected structure of extreme waves in a Gaussian sea. Part II: SWADE scanning radar altimeter measurements. J. Phys. Oceanogr. 23 (10), 2297–2309.

Rapp, R.J., Melville, W.K., 1990. Laboratory measurements of deep-water breaking waves. Philos. Trans. Roy. Soc. Lond. A Math. Phys. Eng. Sci. 331 (1622), 735–800.

Schmittner, C., Kosleck, S., Hennig, J., 2009. A phase-amplitude iteration scheme for the optimization of deterministic wave sequences. In: Proceedings of the International Conference on Offshore Mechanics and Arctic Engineering, vol. 6. OMAE, pp. 653–660.

Stagonas, D., Buldakov, E., Simons, R., 2014. Focusing unidirectional wave groups on finite water depth with and without currents. In: Proceedings of the 34th International Coastal Engineering Conference (ICCE), Seoul, South Korea.

Sutherland, J., Evers, K.U., 2013. Foresight study on the physical modelling of wave and ice loads on marine structures. In: Proceedings of the 35th IAHR World Congress. IAHR, Chengdu, China.

Swan, C., Taylor, P., Van Langen, H., 1997. Observations of wave-structure interaction for a multi-legged concrete platform. Appl. Ocean Res. 19 (5–6), 309–327.

Taylor, P., Williams, B., 2002. Wave statistics for intermediate depth water – NewWaves and symmetry. In: Proceedings of the International Conference on Offshore Mechanics and Arctic Engineering, vol. 2. OMAE, pp. 629–634.

Tian, Z., Perlin, M., Choi, W., 2012. An eddy viscosity model for two-dimensional breaking waves and its validation with laboratory experiments. Phys. Fluids 24, 036601.

Tromans, P.S., Anatruk, A., Hagemeijer, P., 1991. New model for the kinematics of large ocean waves application as a design wave. In: Proceedings of the First International Offshore and Polar Engineering Conference, pp. 64–71.